



## Optimization of extraction protocols for microplastics analysis in lipid-rich food matrices by experimental design

Laura Sforzi<sup>a</sup>, Saul Santini<sup>a</sup>, Serena Orlandini<sup>b</sup>, Costanza Scopetani<sup>a,c</sup>, Chiara Sarti<sup>a</sup>, Tania Martellini<sup>a</sup>, Sandra Furlanetto<sup>b</sup>, Alessandra Cincinelli<sup>a,\*</sup>

<sup>a</sup> Department of Chemistry "Ugo Schiff", University of Florence, Via della Lastruccia 3-13, Sesto Fiorentino 50019, Italy

<sup>b</sup> Department of Chemistry "Ugo Schiff", University of Florence, Via U. Schiff 6, Sesto Fiorentino 50019, Italy

<sup>c</sup> Department of Chemical and Geological Sciences, University of Modena and Reggio Emilia, Via Campi 103, Modena 41125, Italy

### ARTICLE INFO

#### Keywords:

Carbonyl index  
Experimental design  
Food safety  
Micro-FTIR  
Plastic

### ABSTRACT

The presence of microplastics (MPs) in food raises concerns about human exposure through ingestion. Reliable identification of MPs in lipid-rich matrices remains challenging due to inefficient digestion and spectral interference during Fourier-Transform Infrared (FTIR) spectroscopic analysis. A Design of Experiments (DoE) approach was applied to optimize MP extraction protocols in fish at different lipid content, such as salmon, tuna, and cod. Recovery percentage and carbonyl index (CI) were used as proxies for extraction efficiency and residual lipid interference in absorbance spectra. Screening Design and Response Surface Methodology allowed evaluation of digestion time, temperature, and solvent type effects. Specific optimal conditions were identified as: Lipase at 60°C for 30 h for salmon, 10% KOH at 45°C for 40 h for tuna, and 10% KOH at 55°C for 36 h for cod, achieving high recoveries and low CI values together with reliable chemical characterization. Analysis of real fish samples confirmed MPs contamination, with 42–57% of the total items confidently characterized, with abundances ranging 0.7–2.9 items/g of dry weight and fibers as the dominant morphology. The effectiveness of DoE for optimizing MPs extraction in complex food matrices was demonstrated, and highlighting the need for matrix-specific analytical protocols to support harmonized food safety assessments.

### 1. Introduction

The pervasive microplastics (MPs) contamination is a growing key concern because they pose risks for marine and terrestrial ecosystems, and human health. These polymeric particles have been detected in all environmental compartments (water, soil, air) and are capable of reaching humans through contaminated food, dust and water (Padervand et al., 2020). Among the potential exposure routes, ingestion is considered a relevant pathway for humans, evidencing the urgency for regulation and toxicity assessment.

Recent studies confirm MPs presence in a wide range of food and drinks, from seafood (such as fish, shrimp, and bivalves) (Ferrante et al., 2022; von Friesen et al., 2019), dairy products (Abedi et al., 2025), bottled water (Mehn et al., 2025), and beverages (Socas-Hernández et al., 2024), entering directly through source/environmental contamination (i.e. fish ingesting plastic), or indirectly through diets rich in contaminated products, or from packaging materials release. Human exposure to MPs is no longer sporadic but constant through air and

dietary intake, demonstrated by their detection in human blood, lungs, and placenta. This widespread exposure may contribute to chronic health issues, including gut problems, inflammatory responses, cardiovascular and circulatory disorders (Enyoh et al., 2020; Leslie et al., 2022). MPs can also act as vectors for persistent organic pollutants (POPs) and heavy metals, thereby amplifying their toxicological potential (Bridgeman et al., 2025; Pironti et al., 2021).

The evidence of human exposure to MPs through the food chain, especially seafood, and the potential threat to consumers have prompted the European Food Safety Authority (EFSA) to call for the development and standardization of analytical methods to reliably identify and quantify MPs. Broader data sets are also needed for a more comprehensive assessment of the risk to human health and for the development of evidence-based food safety regulations (Food Safety Authority, 2016). In 2025, per capita seafood consumption in the EU has reached approximately 25 kg/person/year total, with Portugal recording the highest consumption rate at 53.6 kg per capita and inland countries such as Hungary with much lower rates (around 6.6 kg) (EUMOFA, 2025).

\* Corresponding author.

E-mail address: [alessandra.cincinelli@unifi.it](mailto:alessandra.cincinelli@unifi.it) (A. Cincinelli).

<https://doi.org/10.1016/j.jfca.2026.109306>

Received 10 March 2026; Received in revised form 4 June 2026; Accepted 9 June 2026

Available online 10 June 2026

0889-1575/© 2026 The Authors. Published by Elsevier Inc. This is an open access article under the CC BY-NC-ND license (<http://creativecommons.org/licenses/by-nc-nd/4.0/>).

Top consumed species by volume in the EU are, in decreasing order, tuna, salmon and cod, followed by shrimp and Alaska pollock. The commonly employed methods for MPs extraction from edible fish, including muscles, livers, and gastrointestinal tracts, consist in a primary extraction method by digestion (i.e. alkaline, oxidative, enzymatic), eventually followed by density separation, vacuum filtration and identification (Expósito et al., 2022; Mistri et al., 2022; von Friesen et al., 2019). The extracted particles are confirmed as plastics using spectroscopic techniques, most commonly Fourier-Transform Infrared (FTIR) spectroscopy (58%) and Raman spectroscopy (8–14%) (Vasudeva et al., 2025). The accuracy of MPs identification in lipid-rich fish tissues, such as muscles, critically depends on overcoming spectral interference from residual organic matter, primarily lipids and proteins, that can persist after digestion procedures (Dawson et al., 2020). These residuals generate signals that overlap with polymer-specific vibrational modes, frequently leading to false positives (i.e. proteins misidentified as polyamide), or false negatives by masking polymer peaks and underestimation (Silva et al., 2022). Therefore, the development of effective MPs extraction protocols for lipid-rich seafood matrices is considered the most critical technical prerequisite for accurate MPs quantification and identification. Such protocols must ensure that samples are “clean” enough for spectroscopic analysis without degrading the polymers. To address these challenges, this study applies, for the first time, the Design of Experiments (DoE) approach to develop and optimize MP extraction protocols suitable for lipid-rich food matrices, like seafood. DoE is a well-established optimization tool in analytical chemistry, with numerous applications ranging from pharmaceutical to environmental and food analysis. Its advantages in the optimization procedures include the ability to obtain high-quality information from a limited number of experiments, the identification of interactions between factors, the development of mathematical models linking variables to responses, and the simultaneous optimization of multiple responses (Eriksson et al., 2008). Several studies have demonstrated the utility of DoE in food analysis (Ferreira et al., 2019), particularly in the development of extraction procedures for compounds of different chemical nature across various matrices (Balli et al., 2020; Cecchi et al., 2024; Marzullo et al., 2022; Zonfrillo et al., 2025), as well as in the optimization of analytical separation methods (Ancillotti et al., 2018). In the field of fish analysis, Freitas et al. applied experimental design within an analytical quality-by-design framework to optimize headspace solid-phase microextraction (HS-SPME) and gas chromatography–mass spectrometry (GC–MS) conditions for the quantification of volatile amines, such as trimethylamine and dimethylamine, key indicators of spoilage in gilthead sea bream (Freitas et al., 2020). Similarly, Silva Oliveira et al. employed DoE through response surface methodology (RSM) to optimize ultrasound-assisted extraction of calcium and iron from fish-based matrices (Silva Oliveira et al., 2026). Anyway, while DoE has been successfully employed in all these contexts, its application in MPs analysis, particularly for the systematic optimization of extraction protocols in lipid-rich fish matrices, remains, to the best of our knowledge, unexplored. The application of DoE represents an advanced methodological approach for the development of MP extraction procedures, allowing the better multivariate combination of factors to be identified for maximizing extraction recoveries and minimizing the carbonyl index (CI), used as a proxy for residual fatty acid contamination affecting the FTIR spectrum quality. The information obtained might be serviceable for future MPs investigations in complex lipid-rich matrices such as seafood, where detection and characterization of MPs will be performed using a dual analytical approach combining stereomicroscopy and micro-FTIR spectroscopy.

## 2. Materials and methods

### 2.1. Chemicals and reagents

30% H<sub>2</sub>O<sub>2</sub> was supplied by J.T. Baker (Gliwice, Poland); 10% KOH

weight/volume (w:v) solution was prepared from KOH solid pellets (VWR Chemicals, Leuven, Belgium); Protease A–01 (subtilisin, EC 3.4.21.62) and Lipase Fe–01 (EC 3.1.1.3) were both purchased from ASA Spezialenzyme GmbH (Wolfenbüttel, Germany). The TRIS-HCl buffer (pH=9) was prepared using tris(hydroxymethyl)aminomethane (Thermo Scientific, California, USA), and 37% HCl was purchased by Carlo Erba Reagents (Cornaredo, Italy). The buffer and the solutions were prepared using VWR H<sub>2</sub>O HiPerSolv CHROMANORM® purchased from VWR Chemicals (Leuven, Belgium). Acetone for glassware cleaning was purchased from Fluke Analytical (Darmstadt, Germany). Glass fiber filters for filtration (GF3 grade, diameter 47 mm) were obtained from CHMLAB Group (Barcelona, Spain). Orange spherical microbeads of polyethylene (PE) in two size ranges, 65–73 μm with density 1.015 g/cm<sup>3</sup>, and 425–500 μm with density 1.00 g/cm<sup>3</sup>, used as internal standards, were purchased from Cospheric Inc (California, USA).

### 2.2. Critical method attributes and internal standard

In the framework of DoE, defining the analytical responses, referred to as Critical Method Attributes (CMAs), is essential for optimizing the extraction and characterization of MPs. In this context, two CMAs have been identified: the recovery percentage (%) and CI. The first one is a fundamental parameter to evaluate the efficiency and accuracy of an analytical protocol, particularly when extraction processes are involved. It is calculated as the ratio between the amount of an internal standard recovered and the known amount of standard added. CI is a key indicator generally used to specifically monitor polymer degradation state (e.g., oxidation) via FTIR spectroscopy, by measuring the ratio between the intensity of the carbonyl absorption peak of the polymer (typically around 1730–1745 cm<sup>-1</sup>), that can arise after degradation, and a stable reference band of the polymer backbone (e.g., CH<sub>2</sub> bending, 1450–1470 cm<sup>-1</sup> in the case of PE) that does not change with polymer alteration (Almond et al., 2020). A high value of CI reflects a high degradation rate of the polymer. Additionally, carbonyl is also a typical group present in fatty acids, thus carbonyl signals serve also as a key tool for monitoring the presence of stubborn matrix residues after digestion. In the spectroscopic characterization of MPs, ensuring surface cleanliness is crucial because residual organic matter, particularly lipophilic substances, has high specific surface areas that can mask the true polymer signal. In the absence of a standardized global protocol for calculating the CI value, using either peak height or area, peak height was chosen for this study. Since the carbonyl region is non-specific and may include contributions from multiple functional groups, further complicating interpretation in complex matrices, the analysis was not based exclusively on the carbonyl region (Gomes et al., 2024). The entire FTIR spectral profile was systematically evaluated to distinguish between PE samples subjected to potential oxidation and those affected by residual lipid contamination. If polymer degradation had occurred, the spectral changes would have been localized primarily in the carbonyl region, whereas the characteristic bands of PE remain consistent with the polymer's backbone. In contrast, samples containing residual lipid layers exhibited a more pervasive alteration of the spectral profile, including an increase in intensity in the carbonyl region accompanied by broader changes in the CH stretching region (typically around 2800–3000 cm<sup>-1</sup>), and an overall baseline distortion.

Currently, there are no certified reference materials (CRMs) available for MPs analysis in real food matrices. Although several commercial materials have been introduced for method development, these materials are generally composed of particles embedded in simple carriers or in powder form and are not suitable for complex food systems, particularly lipid-rich samples. For this reason, single-use standard microbeads (SMs) were manually prepared. Using tweezers and metal spatulas, n = 20 SMs with a diameter of 450–500 μm and approximately 0.003 g of SMs with a diameter of 63–75 μm were added to 1.5 mL Eppendorf microtubes, which were then sealed and numbered. Therefore, the larger SMs were used to assess recovery (%), while the smaller were used

to calculate the CI.

### 2.3. Sample selection

Fish fillets were purchased from a local market located in Florence (Italy). Selecting salmon (*Salmo salar*), tuna (*Thunnus albacares*), and cod (*Gadus morhua*) for MP extraction is highly strategic for their different lipid contents and because they represent the main exposure routes for the Mediterranean and broader EU populations. The lipid content of each fish species was determined gravimetrically ( $n = 3$ ), obtaining values of  $32.5 \pm 0.0\%$  for salmon,  $11.7 \pm 0.1\%$  for tuna, and  $1.3 \pm 0.3\%$  for cod. Information on fish collection, moisture and lipid content, are shown in Table S1. All fillet samples were freeze-dried prior to digestion protocols.

### 2.4. Optimization of the extraction protocols

The Critical Method Parameters (CMPs), i.e., factors within the extraction method that are hypothesized to significantly influence CMAs, were chosen as follows: temperature (*Temp*) and time (*time*), as quantitative factors, and solvent type (*Solv*), as qualitative factor. The experimental domain explored by the DoE was: *Temp*, 40–60 °C; *time*, 24–72 h; and *Solv*, H<sub>2</sub>O<sub>2</sub>, 10% KOH w:v, Lipase, and Protease. The analysis and subsequent optimization were conducted in parallel for the three fishes, based on the different information obtained in relation to lipid content. The final optimized conditions for MPs extractions, i.e., the working points, were: 60 °C for 30 h with Lipase for salmon; 45 °C for 40 h with 10% KOH w:v for tuna; 55 °C for 36 h with 10% KOH w:v for cod (Table S2). The working point conditions were also applied to assess the real environmental MPs contamination of the fish fillet samples. The fishes were extracted and analyzed in triplicate.

Approximately 2.5 g of freeze-dried tissue was weighed into a glass beaker, to which a randomly selected Eppendorf microtube containing SMs was added and mixed. Then, the extraction solvent was added at 1:10 w:v ratio, and the beaker was sealed with aluminum foil. 10% KOH and 30% H<sub>2</sub>O<sub>2</sub> solutions could be used directly, whereas the enzymatic solutions required the addition of a buffer system (i.e., Tris-HCl) to adjust the solution pH to 9. In this case, 5 mL of pure enzyme was added, along with 20 mL of buffer solution, to achieve a total extraction solvent volume of 25 mL. The digestion process was performed in a thermostatic stove (Memmert UM500, Germany) at temperature and time defined by the experimental plans obtained by DoE (Tables S2). The sample was then removed and kept at room temperature until digestion was complete. Then, the solution was transferred to a glass vial and centrifuged at 3000 rpm for 5 min (Neya 10R, Remi Elektrotechnik, India) to separate undigested organic matter. The supernatant was then filtered through a Buckner funnel using a vacuum pump, on glass fiber filters. In some cases, filtration required separation of the solutions across multiple filters, given the high load of undigested lipids/organic matter. The Buckner funnel, beaker, and glass vial were also rinsed with HPLC grade water to ensure recovery of all SMs.

### 2.5. Spectroscopy analysis

Filters were analyzed using a stereomicroscope Leica S9iper equipped with a FLEXACAM C1 digital camera, while chemical characterization and CI calculation were assessed using a 2D imaging FTIR Spectroscopy equipped with a Cary 620–670 FTIR microscope, a 128 × 128 FPA (Focal Plane Array) detector, and two objectives, a 15x (visible, IR) and a 4x (visible) (Agilent Technologies, Waldbronn, Germany). Larger SMs were counted for recovery (%) evaluation, while the smaller were characterized to evaluate the digestion efficiency. Each spectrum was acquired in reflectance mode, with a spectral resolution of 8 cm<sup>-1</sup>, by averaging 128 scans in a spectral range between 3900 and 900 cm<sup>-1</sup>. A background spectrum was acquired each day of analysis using a gold reference plate, and the instrumental parameters were

configured before each session. A 4x magnifying lens was used to acquire visible images of the SMs, while a 15x magnifying lens was used in IR light to acquire spectra and imaging maps. The items were acquired in 2D false-color maps with a surface area of 128 × 128 pixels (700 × 700 μm<sup>2</sup>, where each pixel is 5.5 × 5.5 μm<sup>2</sup>). The 2D maps represented the intensity of the characteristic bands of the polymer studied, and their color scale shows an increase in the absorbance of the bands in the following order: blue < green < yellow < red. Agilent Resolution Pro software (Agilent Technologies) was used to analyze the spectra. The absorption bands and the complete spectrum profile of the SMs were compared with the reference spectra of PE and the clean SMs, while for the real contamination the identified fibers and fragments were compared with the reference spectra reported in the literature (Jung et al., 2018).

### 2.6. Contamination control

Contamination control was performed throughout all digestion and extraction procedures, sample analysis, and standard preparation. Blank controls were performed by filtering HPLC grade water through clean filters at the beginning, middle, and end of each batch, while atmospheric contamination was monitored by placing a wet filter under the hood during filtration. Aliquots of pure solvent and solutions were filtered before use to ensure cleanliness. No traces of contamination were found in any of the blanks analyzed. Only HPLC-grade water and acetone were used to clean laboratory surfaces and benches. All glassware and metal equipment were soaked overnight in a soapy solution and rinsed with HPLC-grade water and acetone, covered with aluminum foil, and stored under a fume hood until use. Operators always wore bright yellow polypropylene laboratory coats, shoe covers, and blue nitrile gloves throughout sample handling to avoid self/cross-contamination. The characteristics of the laboratory coats, including the type of polymer, color, and expected release profile, made it possible to distinguish yellow polypropylene fibers potentially resulting from self-contamination from MPs of environmental origin. Consequently, whenever items with these properties were detected, they were excluded from the final abundance calculations to avoid overestimation.

### 2.7. Data analysis and software

NemrodW software (NemrodW, LPRAI sarl, Marseille, France) was used in the screening phase for planning the asymmetric screening matrix and for related data treatment to identify which factors significantly impact the extraction. MODDE Pro Version 13.1 software (Sartorius Data Analytics, Göttingen, Germany) was used for generating Face Centered Design (FCD), drawing contour plots and defining the optimal conditions. The DoE experimental runs were performed in randomized order.

## 3. Results and discussion

In this study, the DoE approach was applied to optimize protocols for the extraction and analysis of MPs in food matrices with varying lipid contents. This study focused on two main goals: maximizing recovery (%) and minimizing CI. Similar studies using a DoE-based approach to investigate and optimize parameters for MPs extraction have not yet been conducted, so the extraction protocols developed were effectively adapted to each fish species.

### 3.1. Screening phase

During the screening phase, the influence of the three CMPs (*time*, *Temp*, and *Solv*) on the CMAs was systematically evaluated. Several studies have shown that temperature, time, and the type of solvent significantly influence the removal of organic matter during the extraction of microplastics from environmental matrices (Akhbarizadeh

et al., 2025; Cheng et al., 2025; Huang et al., 2025; Larrea et al., 2025). Therefore, these parameters were considered key factors to evaluate. Other potentially affecting steps in the sample preparation workflow (e.g., centrifugation, filtration, and spiking) were performed under standardized conditions for all samples to minimize variability and prevent unintended biases in the results. According to literature data and to the results of previous experiments performed in our laboratory (data not shown), H<sub>2</sub>O<sub>2</sub>, alkaline digestion with KOH, and enzymatic solutions are the most commonly used solvents for MPs extraction from foods (Da Costa Filho et al., 2021; Löder and Gerdts, 2015; S. Monteiro et al., 2022; Santini et al., 2024). These reagents, combined with time and temperature, act as the main drivers for digestion efficiency and polymer recovery. In this study, *Temp* and *time* were investigated at three levels, while *Solv* was investigated at four levels in a suitable experimental domain, as shown in Table S2. The Free-Wilson model (Lewis et al., 1998) assumed to describe the relationship between the CMPs and the CMAs is presented below:

$$y = b_0 + b_{1A} * (X_{1A}) + b_{1B} * (X_{1B}) + b_{2A} * (X_{2A}) + b_{2B} * (X_{2B}) + b_{3A} * (X_{3A}) + b_{3B} * (X_{3B}) + b_{3C} * (X_{3C})$$

where  $y$  is the response,  $b_0$  is the constant term or the intercept of the model,  $X_1$  is *time*,  $X_2$  is *Temp*,  $X_3$  is *Solv*. For each CMP, the number of coefficients in the model corresponds to the number of investigated levels minus one. A 3<sup>2</sup>4<sup>1</sup>/16 asymmetric screening matrix was generated by the NemrodW software for evaluating the effects of the distinct levels of the CMPs on the CMAs (Table 1). This experimental matrix allows the identification of significant factors and the definition of a suitable experimental domain for the subsequent Response Surface Methodology (RSM) phase. The established targets were set for the CMAs as follows: recovery  $\geq 70\%$ , ensuring that the method is efficient enough for quantitative environmental monitoring, and CI  $\leq 0.5$ , ensuring that the chemical signature of the polymer is preserved well

enough for accurate identification via micro-FTIR. Previous work reports an overall average recovery of approximately 86% across different environmental matrices, with lower values for complex matrices such as fishmeal (58–70%) (Way et al., 2022). Therefore, 70% represented a realistic and robust benchmark for lipid-rich samples in this study. Concerning CI, threshold values have not yet been standardized and vary depending on the calculation method (Almond et al., 2020). For this reason, a target of  $\leq 0.5$  was selected based on RSM results and the observed ranges for the target species (Tables S3–S5) to ensure high spectroscopic quality and effective matrix digestion. These values were fixed by considering the lipid content of each fish and the realistic achievable digestion level using the selected solvents, to obtain a good compromise for all the CMAs. A total of 48 experiments, 16 for each of the three fishes, were conducted.

The models obtained for each CMA demonstrated statistical significance according to ANOVA (Table S6). Table S7 presents the coefficients of the Free-Wilson model together with standard deviation and corresponding p-values, indicating their statistical significance, while Table S8 reports the estimated differences in weights between two levels, along with the corresponding standard deviation and p-values, providing an indication of the significance of the terms. The mathematically calculated coefficient values can be more effectively visualized and interpreted through the graphical analysis of effects reported in Fig. 1, which provides a visual representation of how a change of level of the CMPs influences the target CMAs. The plots shown on the left (Fig. 1a, c, e, g, i, k) highlight whether the effect observed on the CMAs is statistically significant when transitioning between different factor levels. When a change in factor level produces a statistically significant effect on the CMA, the corresponding bar is colored in orange. The plots displayed on the right (Fig. 1b, d, f, h, j, l) highlight the effect associated with each individual level of the CMPs on the CMAs, and the three (*time*, *Temp*) or four (*Solv*) investigated levels are represented using distinct

**Table 1**

Asymmetric screening matrix used in the screening phase, together with CMAs values measured for salmon, tuna, and cod.

| No. experiment | <i>Temp</i> (°C) | <i>time</i> (hours) | <i>Solv</i>                   | Salmon       |       | Tuna         |       | Cod          |       |
|----------------|------------------|---------------------|-------------------------------|--------------|-------|--------------|-------|--------------|-------|
|                |                  |                     |                               | Recovery (%) | CI    | Recovery (%) | CI    | Recovery (%) | CI    |
| 1              | 40               | 24                  | H <sub>2</sub> O <sub>2</sub> | 30           | 0.773 | 25           |       | 70           | 2.714 |
| 2              | 40               | 48                  | KOH                           | 5            | 0.139 | 90           | 0.219 | 85           | 0.072 |
| 3              | 40               | 72                  | Lipase                        | 85           | 1.196 | 65           | 0.391 | 75           | 0.149 |
| 4              | 40               | 24                  | Protease                      | 40           | 1.480 | 85           | 8.639 | 65           | 3.000 |
| 5              | 50               | 24                  | KOH                           | 10           | 0.946 | 70           | 0.663 | 100          | 0.045 |
| 6              | 50               | 48                  | H <sub>2</sub> O <sub>2</sub> | 95           | 0.866 | 80           | 0.106 | 95           | 0.040 |
| 7              | 50               | 72                  | Protease                      | 75           | 2.769 | 60           | 0.212 | 80           | 3.000 |
| 8              | 50               | 24                  | Lipase                        | 70           | 0.361 | 60           | 0.677 | 75           | 0.020 |
| 9              | 60               | 24                  | Lipase                        | 60           | 0.413 | 55           | 0.204 | 95           | 0.066 |
| 10             | 60               | 48                  | Protease                      | 55           | 2.769 | 75           | 0.230 | 100          | 3.000 |
| 11             | 60               | 72                  | H <sub>2</sub> O <sub>2</sub> | 90           | 1.008 | 65           | 8.639 | 35           | 0.458 |
| 12             | 60               | 24                  | KOH                           | 75           | 0.154 | 80           | 1.439 | 100          | 0.022 |
| 13             | 40               | 24                  | Protease                      | 35           | 1.201 | 80           | 0.115 | 75           | 3.000 |
| 14             | 40               | 48                  | Lipase                        | 55           | 1.371 | 70           | 0.588 | 85           | 0.434 |
| 15             | 40               | 72                  | KOH                           | 5            | 1.051 | 55           | 0.125 | 70           | 0.085 |
| 16             | 40               | 24                  | H <sub>2</sub> O <sub>2</sub> | 45           | 0.938 | 30           | 0.023 | 55           | 2.867 |
|                |                  |                     |                               |              |       |              | 0.140 |              |       |

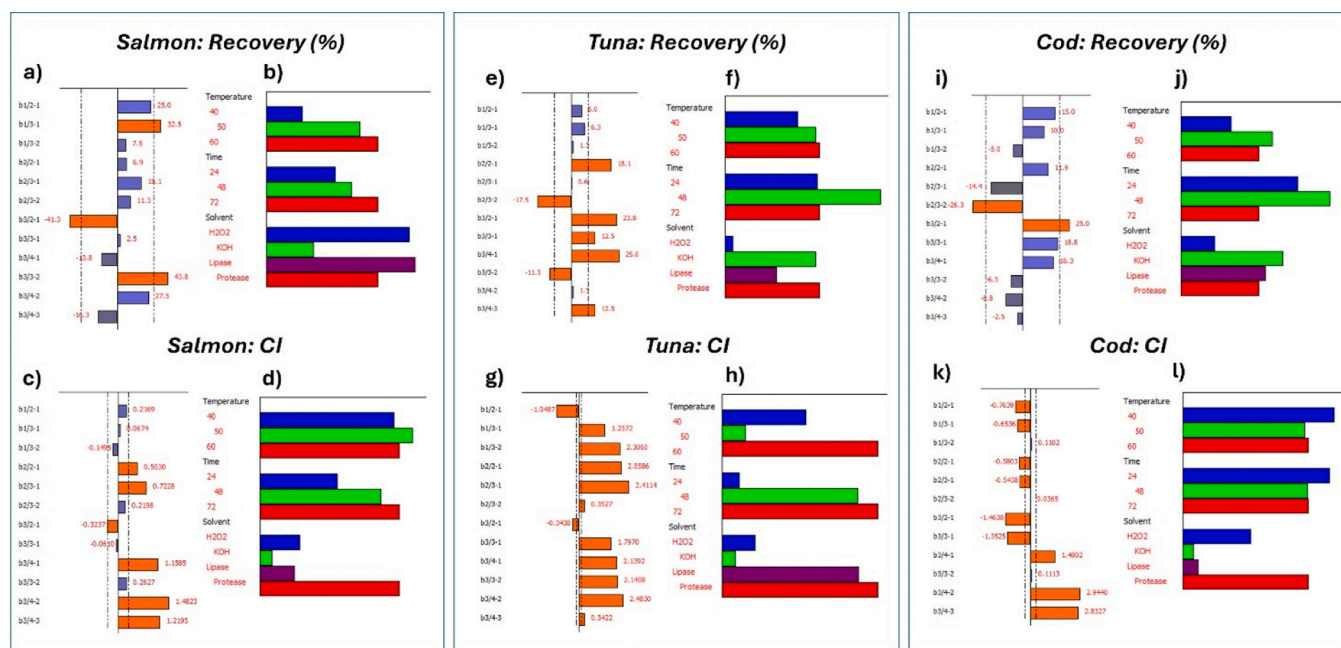


Fig. 1. Screening graphical analysis of effects for each CMA.

colors (blue, green, red, and purple). The length of each bar reflects the magnitude of the effect on the corresponding CMA.

Based on the results reported in Fig. 1, it was possible to identify the specific CMPs settings that led to maximizing recovery and minimizing CI. For salmon, the key optimization conditions for maximizing recovery were obtained at medium to high *Temp*, while changes of this factor did not have a significant impact on CI value. On the contrary, the best conditions for minimizing CI corresponded to shorter digestion *time*, while this factor was not found significant on recovery. The suitable *Solv* were proven to be H<sub>2</sub>O<sub>2</sub> or Lipase for maximum recovery, and KOH or Lipase/H<sub>2</sub>O<sub>2</sub>, with no statistical difference between the two, for minimum CI. However, H<sub>2</sub>O<sub>2</sub> resulted in a wider variability in recovery (measured values ranged from 30% to 95%), whereas Lipase provided a more consistent range (measured values from 55% to 85%). Moreover, none of the experiments performed with H<sub>2</sub>O<sub>2</sub> yielded satisfactory CI values, whereas in the case of Lipase, two experiments (no. 8 and no. 9) resulted in CI values below 0.5. In addition, from a practical perspective, enzymatic treatment with Lipase is generally more selective, reducing the risk of polymer degradation or alteration compared to oxidative treatments such as H<sub>2</sub>O<sub>2</sub>, supporting the choice of lipase as the preferred option. Therefore, Lipase was selected to be the most suitable *Solv* for salmon after the screening phase, representing the best compromise between CMAs.

Considering tuna, it was found that each CMP exerted a strong effect on the responses, apart from *Temp* on recovery. It was clear that *Solv* played a fundamental role, meaning that the chemical reaction of the solvent is crucial for achieving digestion, with KOH proving to be the most effective for simultaneously maximizing recovery and minimizing CI. The best CI results were obtained at medium *Temp* (50 °C), while the lowest *time* level (24 h) contributed the most to CI minimization. On the other hand, the medium *time* level (48 h) proved to have a recovery-related impact leading to the maximization of this response.

For cod, the best extraction for recovery was achieved using low to medium *time*, whereas medium to high *times* were more suitable for CI minimization. Medium-high *Temp* values were preferred for minimizing CI, while recovery did not appear to be affected by this factor. KOH proved to be the most effective for both maximizing recovery and minimizing CI for this species.

The screening phase provided a rational basis for defining the

experimental domain to be explored in the subsequent RSM phase, which was tailored to each fish type. Based on the screening findings, the Lipase enzymatic solution was selected for salmon and the KOH solution for tuna and cod, as these solvents represented the most effective compromise for achieving acceptable recoveries and CI values. The experimental domains of the remaining two factors, i.e., *Temp* and *time*, were adjusted accordingly for each species. The experimental conditions investigated by RSM are summarized in Table S2.

### 3.2. Response surface methodology

In this study, RSM was employed to draw a map of the predicted responses all throughout the experimental domain, thereby supporting the identification of optimal operating conditions for each species of fish. A quadratic model linking the CMPs to the CMAs was hypothesized as the following

$$y = \beta_0 + \beta_1 x_1 + \beta_2 x_2 + \beta_{11} x_1^2 + \beta_{22} x_2^2 + \beta_{12} x_1 x_2 + \varepsilon$$

In this model the CMPs are indicated by  $x_1$  (*Temp*) and  $x_2$  (*time*). The model includes the intercept ( $\beta_0$ ), the linear terms ( $\beta_1$  and  $\beta_2$ ), the quadratic terms ( $\beta_{11}$  and  $\beta_{22}$ ) and the first-order interaction term ( $\beta_{12}$ ), while  $\varepsilon$  represents the experimental error.

An FCD was used to estimate the coefficients of the quadratic model. The experimental plans with the obtained responses are shown in Table S3, S4 and S5 for salmon, tuna and cod, respectively. Suitable mathematical transformations of the responses were performed as indicated in Table S9 and the models were refined by deleting non-significant interaction and quadratic terms. The quality parameters of the model were represented by the coefficient of determination  $R^2$  and the coefficient of prediction variation  $Q^2$ .  $R^2$  represents the fraction of the variation of the response explained by the model and it is calculated as  $R^2 = SS_{\text{regr}}/SS_{\text{tot}} = 1 - SS_{\text{res}}/SS_{\text{tot}}$ , where  $SS_{\text{tot}}$  is the total sum of squares,  $SS_{\text{regr}}$  is the regression sum of squares,  $SS_{\text{res}}$  is the residual sum of squares. The coefficient of prediction variation  $Q^2$  represents the fraction of the total variation of the response that can be predicted in the model and it is calculated as  $Q^2 = SS_{\text{tot}} - \text{PRESS}/SS_{\text{tot}}$ , where PRESS is the Predicted Residual Error Sum of Squares, which is calculated by leave-one-out cross-validation. This parameter estimates the predictive ability of the model, representing a measure of how well the model will

predict the responses for new experimental conditions (Eriksson et al., 2008).

All the models presented acceptable or good quality parameters in terms of coefficient of determination  $R^2$  and  $Q^2$  (Table S9) (Eriksson et al., 2008), and in any case they were found valid and significant by ANOVA (Table S10). An important exception was represented by the model for Cod CI, which exhibited inadequate quality characteristics with regard to both fitting and prediction. For this CMA, the RSM framework did not yield a good predictive model, highlighting that the generalizability of multivariate optimization for such complex systems may depend on the specific matrix–response combination. For the present proof-of-concept study, this issue was addressed by considering that all CI values measured during RSM were below 0.5 and thus fulfilled the

target throughout the experimental domain, so that further investigation of this response was deemed unnecessary. Anyway, it should be underlined that the matrix- and response- dependent performance of the multivariate approach highlights the need for further applications and studies of DoE-based optimization in complex food systems.

The graphic representation of the coefficients, which provides a visual summary of the magnitude and statistical significance of the model terms, is presented in Figure S1. The length of each bar is proportional to the weight of the coefficient. Several quadratic effects of coefficients were evidenced: firstly, a negative quadratic effect of *Temp* and a positive quadratic effect of *time* on salmon CI; secondly, quadratic effects of *time* on both tuna recovery (positive) and tuna CI (negative); and finally, a positive quadratic effect of *Temp* on cod recovery.

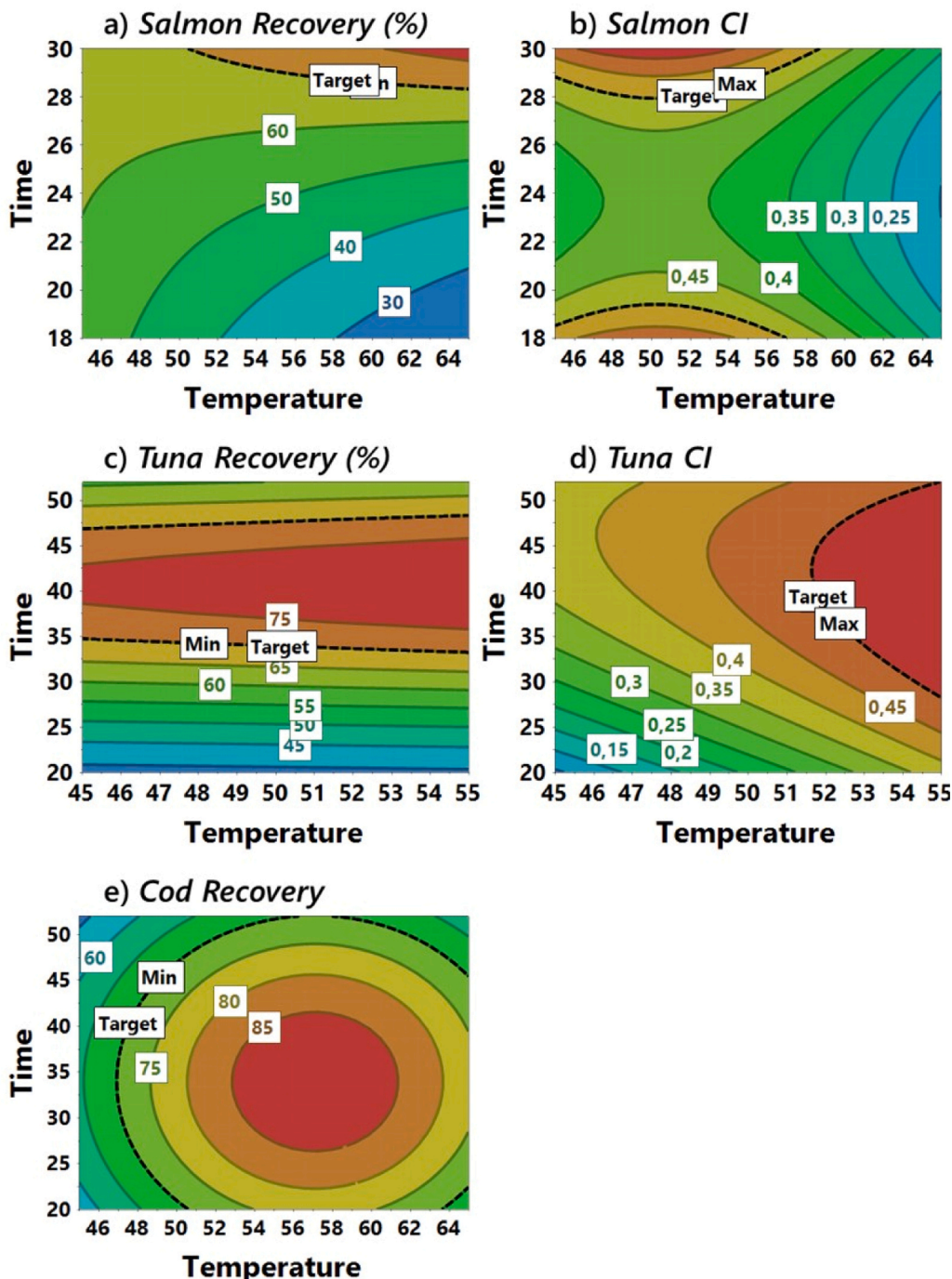


Fig. 2. RSM contour plots of the CMAs obtained plotting *time* vs. *temp*. a) Salmon recovery; b) Salmon CI; c) Tuna recovery; d) Tuna CI; e) Cod recovery.

Fig. 2 reports the RSM contour plots obtained by plotting *time* vs. *Temp*. The maximization of recovery was obtained in the orange-red zones, while the minimization of CI was obtained in the blue zones. With regard to salmon, the recovery was maximized at high levels of *Temp* and *time*, while CI was minimized at high levels of *Temp* and medium levels of *time*. As concerns tuna, the best outcomes for recovery were achieved at medium-high levels of *time*, irrespective of the specific value of *Temp*, while CI was minimized at low levels of both factors. The maximization of cod recovery was obtained in a zone approximately situated at the center of the experimental domain taking in mind that all the CI responses measured in the whole RSM experimental domain were satisfactory.

In order to find the best compromise between the responses, sweet spot approach was used (Eriksson et al., 2008). The sweet spot plots (Figure S2) are generated by overlapping individual CMA contour plots in order to identify the “sweet spot” multidimensional region of the experimental domain where the models predict that all the considered target response criteria are simultaneously satisfied (green color zones). These criteria are based on target thresholds for each CMA, rather than on the maximization or minimization of a single response. MODDE software uses the acceptance range of the responses as specified in the fields minimum, target and/or maximum. For salmon and tuna, sub-regions where only one of the two CMA criteria is met are colored in blue (Figure S2a and S2b). For cod, only the recovery target was taken into account to draw the plot (Figure S2c).

The sweet spot approach does not aim to identify a single optimal point; rather, it defines a robust operating window within which working conditions can be selected (i.e., within the green zone) based on practical considerations, such as reducing extraction time, limiting temperature values, and achieving higher recovery values or lower CI values, as indicated by the individual contour plots. The flexibility of choosing the operating conditions inside the sweet spot represents a key advantage of this approach. Therefore, the selected representative working points for each species were selected as follows: Lipase enzymatic solution at 60 °C for 30 h for salmon, 10% KOH at 45 °C for 40 h for tuna, and 10% KOH at 55 °C for 36 h for cod (Table S2). While specific conditions were not necessary for a 10% KOH solution, the use of lipase normally required optimal catalytic conditions. The effective digestion observed in the salmon matrix at 60 °C for 30 h likely results from a combination of enzymatic and physicochemical effects. For example, the increase in temperature likely promotes the partial denaturation of the matrix's protein components, improving the accessibility of lipid substrates to the solvent (Ahmed Nasef et al., 2021), whereas microbial lipase can maintain residual catalytic activity at higher temperatures (Balan et al., 2012). Furthermore, non-enzymatic factors may be involved, such as delayed chemical hydrolysis in slightly alkaline environments due to the Tris-HCl buffer (Duché & Sanderson, 2024). By applying these conditions, the measured values ( $n = 3$ ) of recovery and CI fulfilled the target requirements: recovery > 70% and CI < 0.5 (Table S11).

Although lipid percentage can be considered a fundamental matrix property in driving CMPs selection, and therefore working point conditions, due to its established influence on digestion efficiency and spectroscopic interference (Da Costa Filho et al., 2021), additional matrix-related factors may also contribute to extraction performance and help explain the observed differences between salmon, tuna, and cod. In particular, variations in tissue structure, protein content, sample integrity, and storage conditions, including freezing and packaging history, can affect both the removal of organic matter and the persistence of interfering residues after digestion. Therefore, the relationship between matrix composition and analytical performance should be considered multifactorial rather than dependent solely on total lipid content. However, the results highlight the importance of adopting matrix-specific optimization strategies when developing extraction protocols for lipid-rich food matrices.

### 3.3. Spectroscopic results and considerations

Examples of SMs' absorbance spectra under the working point conditions are reported in Fig. 3. Although some background noise may still be visible, the FTIR spectra pattern of PE is clearly visible in each sample, even when comparing the samples with the spectrum of the clean polymer (Figure S3). Comparing the spectra obtained under optimized conditions with examples from other digestion carried out with different CMPs (Figure S4), a significant improvement can be noted. Under inefficient conditions, due to residual lipid contamination, poor spectral quality was obtained with broadened absorption bands, corroborated by the visible light maps, preventing reliable chemical characterization. Achieving optimal results was particularly challenging for salmon, especially given its significantly higher lipid content compared to other fishes.

Recovery % and CI did not necessarily show a direct correlation. In the case of salmon, for example, some experimental conditions have resulted in high recovery values but low confidence in CI, and vice versa. The size of SMs can affect their behavior in density separation, by influencing how polymers interact with lipids. Given the hydrophobic nature of most polymers, SMs may preferentially associate with lipids, as also reported by Scopetani et al. (Scopetani et al., 2020). Under such conditions, high recovery may result from particles remaining adhered to lipids, while lower recovery may result from those embedded into the fat fraction, rather than being freely available for spectroscopic analysis. Conversely, chemical characterization is favored under conditions where lipids are largely removed, but residual fat can immobilize particles while simultaneously coating their surface, thus compromising FTIR spectral quality and leading to higher recovery. Indeed, Scopetani et al. observed that plastic particles readily partitioned into the hydrophobic oil phase when oil and water were combined, suggesting a similar behavior of SMs in fish samples (Scopetani et al., 2020). A further limitation is that SMs addition was performed on dried samples to prevent particle loss during drying, although real samples are expected to contain MPs fully embedded within the native matrix. Nevertheless, as organic matter progressively degrades during the digestion stages, fibers and fragments originally entrapped within the tissue may be released into solution, indicating that the use of spiked standards can reasonably simulate this later MPs release phase. Although these mechanisms may explain the observed discrepancy between recovery values and chemical identification performance, further study of the actual MP behavior would be required.

In this context, the efficacy and efficiency of DoE for the optimization of analytical protocols targeting MPs have been demonstrated, and these results provide a solid basis for future investigations aimed at exploring advanced digestion strategies for lipid-rich food matrices. Future studies should focus on implementing more complex approaches, such as the use of solvent mixtures, multi-step digestion protocols, wider temperature and time ranges, and on extending the study to different types of foods.

### 3.4. Real sample analysis

The reliability and applicability of the proposed method were assessed by analyzing the real contamination extent in fish fillet. Samples ( $n = 3$ ) of salmon, tuna, and cod were analyzed following the corresponding procedure for each species of fish, and the obtained results are reported in Table 2. Although MPs are not actually among regulated contaminants in food, studies have demonstrated that the food chain is the primary route of exposure, and the potential effects that may have on human health are concerning (Ziani et al., 2023). MPs were detected in all samples, indicating the ubiquity of MPs as contaminants. Abundances were comparable between tuna and cod,  $2.9 \pm 2.0$  and  $2.7 \pm 2.9$  items/g dry weight (dw), respectively, while salmon showed a lower concentration, at  $0.7 \pm 0.6$  items/g dw. The detection of MPs in all analyzed samples confirms their widespread presence in fish and

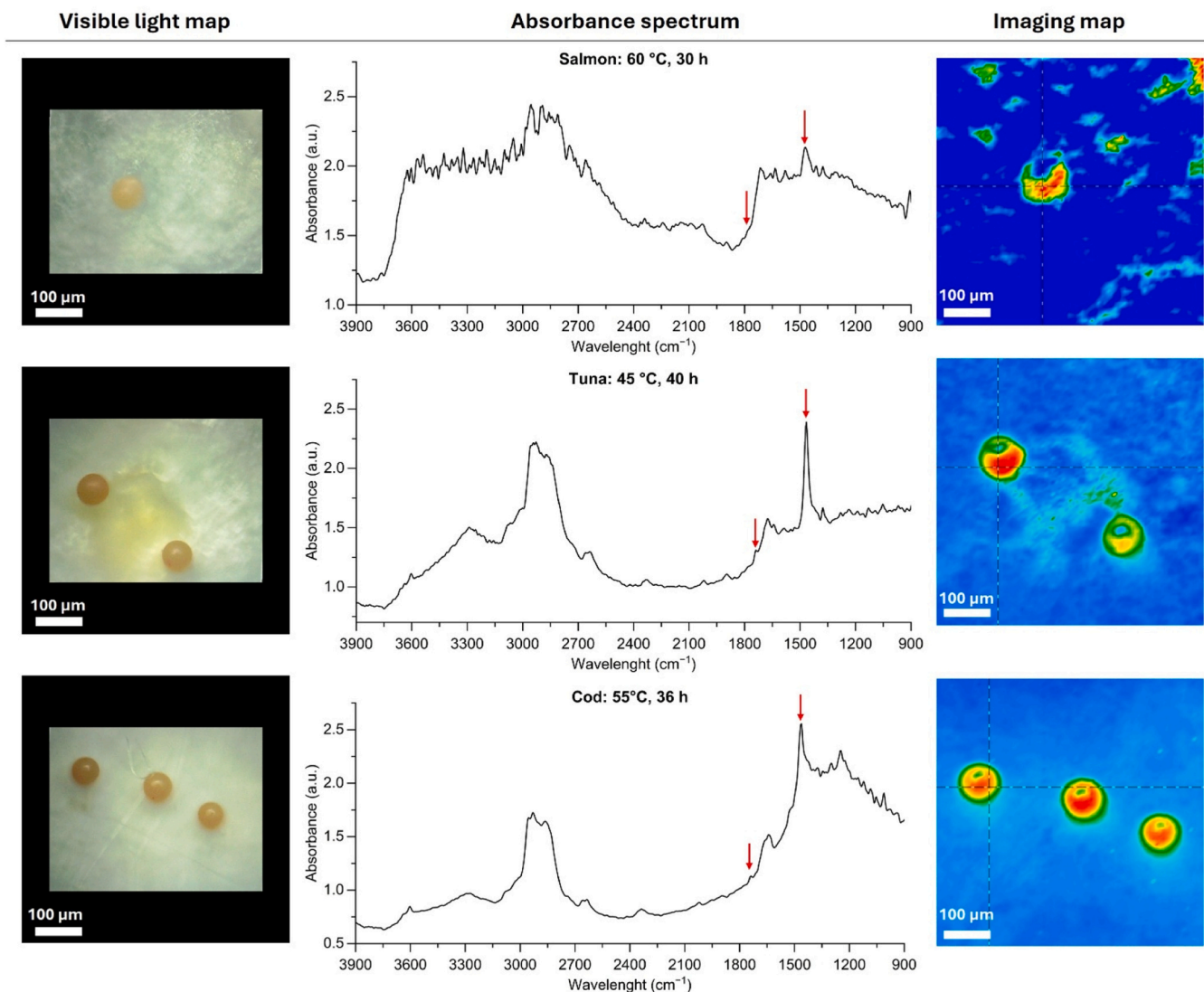


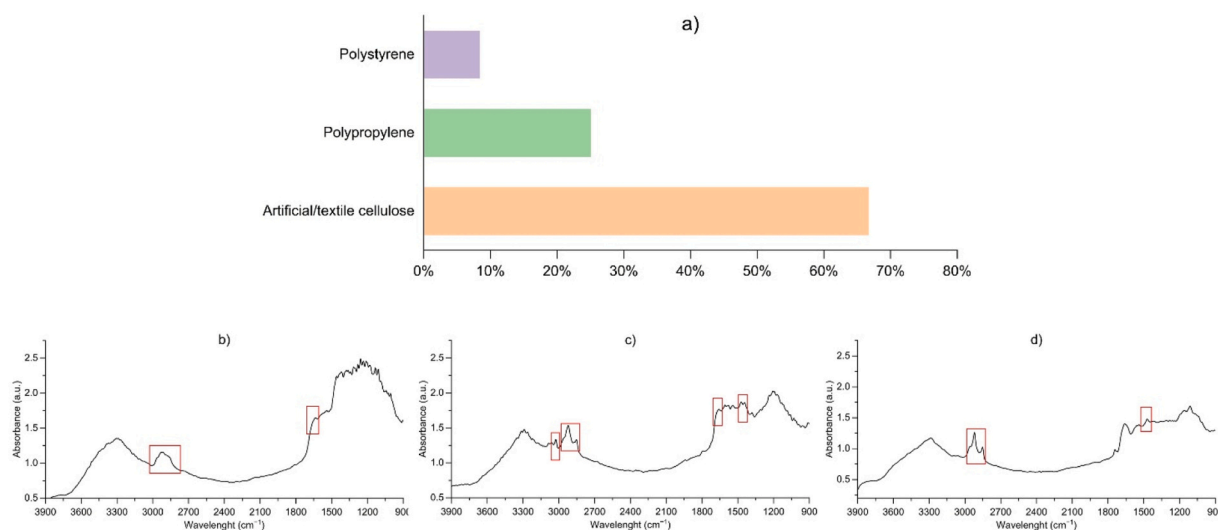
Fig. 3. Visible light maps, imaging maps, and absorbance spectra of standard MBs for salmon, tuna, and cod after digestion optimization. Red arrows indicate the carbonyl group and the polyethylene-specific reference peaks with minimal spectral interference.

Table 2  
MPs abundances (items/g dw,  $n = 3$ ) and characteristics in fish samples.

| Fish sample | Abundance (items/g dw) | Mean size ( $\mu\text{m}$ ) | Morphology (%)              | Colors (%)  |
|-------------|------------------------|-----------------------------|-----------------------------|---|
| Salmon      | $0.7 \pm 0.6$          | $380.0 \pm 178.9$           | Fibers: 80<br>Fragments: 20 | Black: 20<br>Blue: 60<br>Grey: 20   |
| Tuna        | $2.9 \pm 2.0$          | $257.7 \pm 195.0$           | Fibers: 73<br>Fragments: 27 | Black: 41<br>Blue: 18<br>Red: 5<br>Yellow: 14<br>Pink: 4<br>Purple: 4<br>Sky blue: 14                 |
| Cod         | $2.7 \pm 2.9$          | $252.5 \pm 262.8$           | Fibers: 60<br>Fragments: 40 | Black: 30<br>Blue: 25<br>Red: 15<br>Yellow: 5<br>Pink: 5<br>Grey: 10<br>Transparent: 5<br>Sky blue: 5 |

supports previous findings reporting the ubiquity of MPs in marine products (Mistri et al., 2022). Differences between species can be attributed to a combination of factors, including feeding behavior, habitat, and trophic level (Xie et al., 2024). Fiber was the predominant morphology observed in all samples, accounting for 80–60%, while the dominant colors were black (range 20–41%) and blue (range 18–60%).

After counting and classifying the items based on morphological criteria, they were subjected to chemical analysis. The percentage of items that could be confidently characterized was 42% for salmon, 53% for tuna, and 57% for cod, with FTIR spectra showing clear and defined absorption patterns, suitable for chemical characterization (Fig. 4). Since visual identification alone is not sufficient for reliable polymer classification, only chemically confirmed items of synthetic/anthropogenic origin were included in the compositional analyses. This conservative approach likely reduced the total number of items included in the final dataset, but minimized the risk of overestimating contamination due to false-positive identifications. The chemical identification rate was strongly influenced by the intrinsic complexity of the matrix, as well as by sample heterogeneity, which may have prevented the complete removal of interfering substances from some particles prior to spectroscopic analysis. Nevertheless, chemical characterization under optimized conditions yielded acceptable results, supporting the potential



**Fig. 4.** a) Percentage of polymer types, and samples absorbance spectra of b) artificial/textile cellulose, c) polystyrene, and d) polypropylene. The red squares indicate the diagnostic peak that enabled polymeric assignment.

adaptability of the proposed protocols to other food matrices and confirms the importance of tailored sample preparation for reliable spectroscopic analysis. Cellulose of artificial/textile origin was the most abundant polymer found (67%), followed by polypropylene (25%), and polystyrene (8%). Visible light maps of items found are shown in Figure S5.

The morphology, size, and color of the items found were consistent with those typically reported for MPs in seafood (Felline et al., 2022). Items with a cellulose-based composition have been grouped into the “artificial cellulose/textile” category to distinguish them from natural cellulose. Although regenerated cellulose materials are not plastics in the strict sense of polymer classification, they may be included in MPs abundance data, since anthropogenic treatments they have undergone (such as the addition of dyes, UV stabilizers, flame retardants, plasticizers, etc.) (Athey and Erdle, 2022) may result in toxicological impacts similar to those of synthetic fibers, raising concerns about their potential transfer through the marine food web. Although the method was validated using reference PE SMS, it was expected to remain effective for the recovery of cellulose-based fibers, primarily because extraction efficiency had been determined by evaluating the matrix digestion and phase separation processes, rather than based on the specific chemical properties of the target particles. Furthermore, unlike PE, artificial or textile-derived cellulose is less hydrophobic, which could facilitate its recovery during aqueous treatment and filtration steps, and the relatively mild conditions investigated (e.g., avoiding aggressive solvents and extreme temperatures) are unlikely to induce degradation, thereby preserving the structural integrity of the cellulose fibers. The high percentage of cellulose of artificial and/or textile origin suggests a significant contribution of fibers, which are frequently reported in food and environmental samples and may originate from clothing, packaging materials, or environmental sources (Santonicola et al., 2024). Nevertheless, the detection of synthetic polymers such as polypropylene and polystyrene confirms the presence of plastic-derived particles within the analyzed fish samples. Although MPs were detected in all the samples analyzed, a finding that continues to raise concerns about this type of contamination in products intended for human consumption, the samples collected are not necessarily representative of MP levels in fresh fish, given the small sample size and the variability in the fish’s origin, storage methods, and packaging. Although the results demonstrate the effectiveness of the DoE approach in optimizing extraction conditions for the lipid-rich matrix investigated in this study, these results must be interpreted within the context of the specific system evaluated. The optimized parameters are closely matrix-dependent and may not be

directly applicable to other types of foods with different composition (e.g., dry food, meat, dairy products, etc.), such as protein or lipidic content. Nevertheless, the DoE framework provides a robust and systematic strategy for method optimization. The matrix-specific digestion protocols optimized here are designed to provide a methodological workflow applicable to various fish species. By enabling accurate and reproducible quantification and qualification of MPs in complex food matrices, along with reducing methodological variability and uncertainties associated with matrix interference, these protocols can support the design of future monitoring programs and the generation of exposure datasets necessary for risk assessment. In particular, matrix-adapted methods can improve the reliability of estimated intake calculations and help regulatory authorities define evidence-based safety thresholds, such as maximum tolerable levels of MP in fish and seafood intended for human consumption, following a similar approach already applied to other classes of contaminants (e.g., bisphenols, polyfluoroalkyl substances, etc.) (Jia et al., 2025; Junqué et al., 2026).

#### 4. Conclusions

Although MPs are not currently regulated as food contaminants, increasing evidence indicates that dietary intake, particularly through fish consumption, is a major route of human exposure, raising concerns about potential effects on human health. In this study, DoE was applied to optimize an extraction protocol for the characterization of MPs in lipid-rich food products, such as fish. Factors like time, temperature, and solvent type were systematically evaluated carrying out a screening step and subsequently RSM. Detailed information on the digestion processes was progressively recorded through the measurement of the percentage of recovery and the calculation of the CI. The sweet spot was defined for each species of fish, and the optimal conditions were identified as the use of a Lipase enzyme solution at 60 °C for 30 h for salmon, 10% KOH at 45 °C for 40 h for tuna, and 10% KOH at 55 °C for 36 h for cod. Under these conditions, high recovery rates and reliable chemical characterization of MPs were guaranteed. Furthermore, this study highlights how a “one-size-fits-all” approach may not be suitable for complex matrices, such as lipid-rich foods.

In the field of MP analysis, the use of DoE is still unexplored. However, this study represents a proof-of-concept demonstrating the potential of the multivariate approach, showing that it deserves future attention from researchers. Its advantages include the acquisition of a progressive and in-depth knowledge of how different extraction parameters interact with one another, the development of a robust method

and the enhancement of efficiency and resource management, providing insights that could not be obtained using traditional one-factor-at-a-time approaches, such as the application of multi-criteria optimization. On the other hand, whereas the DoE framework proved effective for most responses, particularly for salmon and tuna, its performance appeared as matrix- and response-dependent. This variability underscores the need for more studies focused on DoE-based optimization in complex food systems, across a wider range of matrices, polymer types, and realistic contamination scenarios.

The absence of standardized analytical approaches for the detection and chemical characterization of MPs in different food matrices hinders meaningful comparison between studies and prevents the establishment of regulatory safety thresholds. Moreover, currently available MP chemical risk assessments are largely based on polymer-specific toxicity data and therefore directly depend on reliable chemical characterization. For these reasons, acquiring a broad field of knowledge in the area of MPs-contaminated foods through the implementation of new and feasible methods will support future food safety monitoring and the assessment of MPs-related risks to human health.

### CRedit authorship contribution statement

**Chiara Sarti:** Writing – review & editing, Visualization. **Tania Martellini:** Writing – review & editing, Visualization. **Sandra Furlanetto:** Writing – review & editing, Visualization. **Alessandra Cincinelli:** Writing – review & editing, Writing – original draft, Supervision, Project administration, Funding acquisition, Conceptualization. **Saul Santini:** Writing – review & editing, Data curation. **Serena Orlandini:** Writing – review & editing, Writing – original draft, Validation, Software, Methodology, Conceptualization. **Costanza Scopetani:** Writing – review & editing, Formal analysis. **Laura Sforzi:** Writing – review & editing, Writing – original draft, Validation, Methodology, Investigation, Formal analysis, Data curation, Conceptualization.

### Declaration of Competing Interest

The authors declare that they have no known competing financial interests or personal relationships that could have appeared to influence the work reported in this paper.

### Appendix A. Supporting information

Supplementary data associated with this article can be found in the online version at [doi:10.1016/j.jfca.2026.109306](https://doi.org/10.1016/j.jfca.2026.109306).

### Data Availability

Data will be made available on request.

### References

- Abedi, D., Niari, M.H., Ramavandi, B., De-la-Torre, G.E., Renner, G., Schmidt, T.C., Dobaradaran, S., 2025. Microplastics and phthalate esters in yogurt and buttermilk samples: characterization and health risk assessment. *J. Environ. Health Sci. Eng.* 23 (1), 1–15. <https://doi.org/10.1007/S40201-025-00939-Z>.
- Ahmed Nasef, N., Zhu, P., Golding, M., Dave, A., Ali, A., Singh, H., Garg, M., 2021. Salmon food matrix influences digestion and bioavailability of long-chain omega-3 polyunsaturated fatty acids. *Food Funct.* 12 (14), 6588–6602. <https://doi.org/10.1039/D1FO00475A>.
- Akhbarizadeh, R., Xu, Y.J., Boerner, F., Helm, P.A., Diamond, M.L., 2025. Optimized Extraction Methods for Pristine and Aged Microplastics from Complex Water Samples. *ACS ES&T Water* 5, 3111–3117. <https://doi.org/10.1021/ACSESTWATER.5C00017>.
- Almond, J., Sugumaar, P., Wenzel, M.N., Hill, G., Wallis, C., 2020. Determination of the carbonyl index of polyethylene and polypropylene using specified area under band methodology with ATR-FTIR spectroscopy. *E-Polymers* 20 (1), 369–381. <https://doi.org/10.1515/EPOLY-2020-0041/XML>.
- Ancillotti, C., Orlandini, S., Ciofi, L., Pasquini, B., Caprini, C., Droandi, C., Furlanetto, S., Del Bubba, M., 2018. Quality by design compliant strategy for the development of a liquid-chromatography-tandem mass spectrometry method for the determination of selected polyphenols in Diospyros kaki. *J. Chromatogr. A* 1569, 79–90. <https://doi.org/10.1016/j.chroma.2018.07.046>.
- Athey, S.N., Erdle, L.M., 2022. Are we underestimating anthropogenic microfiber pollution? A critical review of occurrence, methods, and reporting. *Environ. Toxicol. Chem.* 41 (4), 822–837. <https://doi.org/10.1002/ETC.5173>.
- Balan, A., Ibrahim, D., Abdul Rahim, R., Ahmad Rashid, F.A., 2012. Purification and Characterization of a Thermostable Lipase from *Geobacillus thermodenitrificans* IBRL-nra. *Enzym. Res.* 1, 987523. <https://doi.org/10.1155/2012/987523>.
- Balli, D., Bellumori, M., Orlandini, S., Cecchi, L., Mani, E., Pieraccini, G., Mulinacci, N., Innocenti, M., 2020. Optimized hydrolytic methods by response surface methodology to accurately estimate the phenols in cereal by HPLC-DAD: The case of millet. *Food Chem.* 303, 125393. <https://doi.org/10.1016/j.foodchem.2019.125393>.
- Bridgeman, L., Cimbalo, A., López-Rodríguez, D., Pamies, D., Frangiamone, M., 2025. Exploring toxicological pathways of microplastics and nanoplastics: Insights from animal and cellular models. *J. Hazard. Mater.* 490, 137795. <https://doi.org/10.1016/J.JHAZMAT.2025.137795>.
- Cecchi, L., Orlandini, S., Balli, D., Zanon, B., Migliorini, M., Giambanelli, E., Catola, S., Furlanetto, S., Mulinacci, N., 2024. Analysis of volatile hydrocarbons (pentene dimers and terpenes) in extra virgin olive oil: optimization by Response Surface Methodology and validation of HS-SPME-GC-MS method. *J. Agric. Food Chem.* 72, 2813–2825. <https://doi.org/10.1021/acs.jafc.3c07430>.
- Cheng, Y., Wu, Y., Almuhtar, H., Andrews, R.C., 2025. Assessment of microplastic digestion methods in source and treated drinking waters. *Sci. Total. Environ.* 993, 180009. <https://doi.org/10.1016/J.SCITOTENV.2025.180009>.
- Da Costa Filho, P.A., Andrey, D., Eriksen, B., Peixoto, R.P., Carreres, B.M., Ambühl, M.E., Descarrega, J.B., Dubascoux, S., Zbinden, P., Panchaud, A., Poitevin, E., 2021. Detection and characterization of small-sized microplastics ( $\geq 5 \mu\text{m}$ ) in milk products, 11:1 *Sci. Rep.* 11 (1), 24046. <https://doi.org/10.1038/s41598-021-03458-7>.
- Dawson, A.L., Motti, C.A., Kroon, F.J., 2020. Solving a Sticky Situation: Microplastic Analysis of Lipid-Rich Tissue. *Front. Environ. Sci.* 8, 563565. <https://doi.org/10.3389/FENV.S.2020.563565>.
- Duché, G., Sanderson, J.M., 2024. The Chemical Reactivity of Membrane Lipids. *Chem. Rev.* 124 (6), 3284–3330. <https://doi.org/10.1021/ACS.CHEMREV.3C00608>.
- Enyoh, C.E., Shafea, L., Verla, A.W., Verla, E.N., Qingyue, W., Chowdhury, T., Paredes, M., 2020. Microplastics Exposure Routes and Toxicity Studies to Ecosystems: An Overview. *Environ. Anal. Health Toxicol.* 35 (1). <https://doi.org/10.5620/EAHT.E2020004>.
- Eriksson, L., Johansson, E., Kettaneh-Wold, N., Wikström, C., Wold, S., 2008. Design of experiments: principles and application, 3rd ed. MKS Umetrics AB, Umeå, Sweden (<https://search.worldcat.org/title/900729871>).
- EUMOPA. (2025). The EU fish market. <https://doi.org/10.2771/1531521>.
- Expósito, N., Rovira, J., Sierra, J., Gimenez, G., Domingo, J.L., Schuhmacher, M., 2022. Levels of microplastics and their characteristics in molluscs from North-West Mediterranean Sea: Human intake. *Mar. Pollut. Bull.* 181. <https://doi.org/10.1016/j.marpolbul.2022.113843>.
- Felline, S., Piccardo, M., De Benedetto, G.E., Malitesta, C., Terlizzi, A., 2022. Microplastics' Occurrence in Edible Fish Species (*Mullus barbatus* and *M. surmuletus*) from an Italian Marine Protected Area. *Microplastics* 1 (2), 291–302. <https://doi.org/10.3390/microplastics1020021>.
- Ferrante, M., Pietro, Z., Allegui, C., Maria, F., Antonio, C., Pulvirenti, E., Favara, C., Chiara, C., Grasso, A., Omayma, M., Gea, O.C., Banni, M., 2022. Microplastics in fillets of Mediterranean seafood. A risk assessment study. *Environ. Res.* 204, 112247. <https://doi.org/10.1016/J.ENVRES.2021.112247>.
- Ferreira, S.L.C., Silva Junior, M.M., Felix, C.S.A., da Silva, D.L.F., Santos, A.S., Santos Neto, J.H., de Souza, C.T., Cruz Junior, R.A., Souza, A.S., 2019. Multivariate optimization techniques in food analysis - A review. *Food Chem.* 273, 3–8. <https://doi.org/10.1016/j.foodchem.2017.11.114>.
- Food Safety Authority, E., 2016. Presence of microplastics and nanoplastics in food, with particular focus on seafood. *EFSA J.* 14 (6), e04501. <https://doi.org/10.2903/J.EFSA.2016.4501>.
- Freitas, J., Silva, P., Vaz-Pires, P., Câmara, J.S., 2020. A Systematic AQBd Approach for Optimization of the Most Influential Experimental Parameters on Analysis of Fish Spoilage-Related Volatile Amines. *Foods* 9, 1321. <https://doi.org/10.3390/foods9091321>.
- Gomes, R., Fernandes, A.N., Waldman, W.R., 2024. How to Measure Polymer Degradation? An Analysis of Authors' Choices When Calculating the Carbonyl Index. *Environ. Sci. & Technol.* 58 (17), 7609–7616. <https://doi.org/10.1021/ACS.EST.3C10855>.
- Huang, K., Xie, L., Gu, X., Xie, J., Li, J., Gao, S., Ji, R., Zhou, D., 2025. Comprehensive assessment of various digestion protocols for extraction microplastics from organic-rich environmental matrices. *Water Res.* 282, 123935. <https://doi.org/10.1016/J.WATRES.2025.123935>.
- Jia, Y., Jin, W., Yang, S., Li, X., Li, J., Zhang, Y., 2025. Determination of Bisphenol A and its analogues in crayfish by UPLC-MS/MS and the assessment of dietary exposure of adults in Tianjin. *J. Food Compos. Anal.* 137, 106895. <https://doi.org/10.1016/J.JFCA.2024.106895>.
- Jung, M.R., Horgen, F.D., Orski, S.V., Rodriguez, C., Beers, K.L., Balazs, G.H., Jones, T.T., Work, T.M., Brignac, K.C., Royer, S.J., Hyrenbach, K.D., Jensen, B.A., Lynch, J.M., 2018. Validation of ATR FT-IR to identify polymers of plastic marine debris, including those ingested by marine organisms. *Mar. Pollut. Bull.* 127, 704–716. <https://doi.org/10.1016/j.marpolbul.2017.12.061>.
- Junqué, E., Llorca, M., Bautista, A., Barber, J., Dondero, F., Farré, M., Lynch, I., 2026. Assessment of PFAS pollution in fish and water from the United Kingdom and Spain

- and implications for human exposure. *Environ. Pollut.* 390, 127515. <https://doi.org/10.1016/J.ENVPOL.2025.127515>.
- Larrea, G., Elustondo, D., Durán, A., 2025. Extraction Methods of Microplastics in Environmental Matrices: A Comparative Review. *Molecules* 30 (15), 3178. <https://doi.org/10.3390/MOLECULES30153178>.
- Leslie, H.A., van Velzen, M.J.M., Brandsma, S.H., Vethaak, A.D., Garcia-Vallejo, J.J., Lamoree, M.H., 2022. Discovery and quantification of plastic particle pollution in human blood. *Environ. Int.* 163, 107199. <https://doi.org/10.1016/J.ENVINT.2022.107199>.
- Lewis, G.A., Mathieu, D., Phan-Tan-Luu, R., 1998. *Pharmaceutical Experimental Design*, 1st ed.). CRC Press. <https://doi.org/10.1201/9780203508688>.
- Löder, M.G.J., Gerdts, G., 2015. Methodology used for the detection and identification of microplastics—a critical appraisal. *Mar. Anthropog. Litter* 201–227. [https://doi.org/10.1007/978-3-319-16510-3\\_8](https://doi.org/10.1007/978-3-319-16510-3_8).
- Marzullo, L., Ochkur, O., Orlandini, S., Renai, L., Gotti, R., Koshovyi, O., Furlanetto, S., Del Bubba, M., 2022. Quality by Design in optimizing the extraction of (poly) phenolic compounds from *Vaccinium myrtillus* berries. *J. Chromatogr. A* 1677, 463329. <https://doi.org/10.1016/j.chroma.2022.463329>.
- Mehn, D., Bucher, C., Fumagalli, G., Hadri, E., & Gilliland, H. (2025). Analysing microplastics in drinking water. Publications Office of the EU. <https://doi.org/https://data.europa.eu/doi/10.2760/1240697>.
- Mistri, M., Sfriso, A.A., Casoni, E., Nicoli, M., Vaccaro, C., Munari, C., 2022. Microplastic accumulation in commercial fish from the Adriatic Sea. *Mar. Pollut. Bull.* 174. <https://doi.org/10.1016/j.marpolbul.2021.113279>.
- Monteiro, S.S., Rocha-Santos, T., Prata, J.C., Duarte, A.C., Girão, A.V., Lopes, P., Cristovão, T., da Costa, J.P., 2022. A straightforward method for microplastic extraction from organic-rich freshwater samples. *Sci. Total. Environ.* 815, 152941. <https://doi.org/10.1016/J.SCITOTENV.2022.152941>.
- Silva, D.M., Almeida, C.M.R., Guardiola, F., Rodrigues, S.M., Ramos, S., 2022. Optimization of an Analytical Protocol for the Extraction of Microplastics from Seafood Samples with Different Levels of Fat. *Vol. 27, Page 5172 Molecules* 27 (16), 5172. <https://doi.org/10.3390/MOLECULES27165172>.
- Padervand, M., Lichtfouse, E., Robert, D., Wang, C., 2020. Removal of microplastics from the environment. A review. In: *Environmental Chemistry Letters*, 18. Springer, pp. 807–828. <https://doi.org/10.1007/s10311-020-00983-1>.
- Pironti, C., Ricciardi, M., Motta, O., Miele, Y., Proto, A., & Montano, L. (2021). Microplastics in the Environment: Intake through the Food Web, Human Exposure and Toxicological Effects. *Toxics*, Vol. 9, 224, 224. <https://doi.org/10.3390/TOXI9090224>.
- Santini, S., Exposito, N., Sierra, J., Cincinelli, A., Rovira, J., 2024. Set up and validation of a method to analyse microplastics in stool and small intestine samples. *MethodsX* 12. <https://doi.org/10.1016/j.mex.2024.102777>.
- Santonicola, S., Volgare, M., Schiano, M.E., Cocca, M., Colavita, G., 2024. A study on textile microfiber contamination in the gastrointestinal tracts of *Merluccius merluccius* samples from the Tyrrhenian Sea. *Ital. J. Food Saf.* 13 (2). <https://doi.org/10.4081/ijfs.2024.12216>.
- Scopetani, C., Chelazzi, D., Mikola, J., Leiniö, V., Heikkinen, R., Cincinelli, A., Pellinen, J., 2020. Olive oil-based method for the extraction, quantification and identification of microplastics in soil and compost samples. *Sci. Total. Environ.* 733, 139338. <https://doi.org/10.1016/J.SCITOTENV.2020.139338>.
- Silva Oliveira, G., Santos Nunes, L., de Queiroz Vilas Boas Santos, S., Alves Araújo, S., Pereira Contreiras, J., Chaplin Teles de Almeida, M., Silva Santos, M.J., Almeida Bezerra, M., 2026. Multivariate optimization of an ultrasound-assisted extraction method for the determination of calcium and iron in fish samples. *Research* 4, 101239. <https://doi.org/10.1016/j.nexres.2025.101239>.
- Socas-Hernández, C., Miralles, P., González-Sálamo, J., Hernández-Borges, J., Coscollà, C., 2024. Assessment of anthropogenic particles content in commercial beverages. *Food Chem.* 447. <https://doi.org/10.1016/j.foodchem.2024.139002>.
- Vasudeva, M., Warriar, A.K., Kartha, V.B., Unnikrishnan, V.K., 2025. Advances in microplastic characterization: Spectroscopic techniques and heavy metal adsorption insights. *TrAC. Trends Anal. Chem.* 183, 118111. <https://doi.org/10.1016/J.TRAC.2024.118111>.
- von Friesen, L.W., Granberg, M.E., Hassellöv, M., Gabrielsen, G.W., Magnusson, K., 2019. An efficient and gentle enzymatic digestion protocol for the extraction of microplastics from bivalve tissue. *Mar. Pollut. Bull.* 142, 129–134. <https://doi.org/10.1016/j.marpolbul.2019.03.016>.
- Way, C., Hudson, M.D., Williams, I.D., Langley, G.J., 2022. Evidence of underestimation in microplastic research: A meta-analysis of recovery rate studies. *Sci. Total. Environ.* 805, 150227. <https://doi.org/10.1016/J.SCITOTENV.2021.150227>.
- Xie, S., Song, K., Liu, S., Li, Y., Wang, J., Huang, W., Feng, Z., 2024. Distribution and characteristics of microplastics in 16 benthic organisms in Haizhou Bay, China: Influence of habitat, feeding habits and trophic level. *Mar. Pollut. Bull.* 199, 115962. <https://doi.org/10.1016/J.MARPOLBUL.2023.115962>.
- Ziani, K., Ioniță-Mîndrican, C.B., Mititelu, M., Neacșu, S.M., Negrei, C., Moroșan, E., Drăgănescu, D., Preda, O.T., 2023. Microplastics: A Real Global Threat for Environment and Food Safety: A State of the Art Review. *Nutrients* 15 (3). <https://doi.org/10.3390/nu15030617>.
- Zonfrillo, B., Bellumori, M., Digiglio, I., Innocenti, M., Orlandini, S., Furlanetto, S., Khatib, M., Papini, A., Mainente, F., Zoccatelli, G., Mulinacci, N., 2025. Multivariate optimization of ulvan extraction applying Response Surface Methodology (RSM): the case of *Ulva lactuca* L. from Orbetello lagoon. *Carbohydr. Polym.* 354, 123340. <https://doi.org/10.1016/j.carbpol.2025.123340>.